Seismic modeling of fluid substitution in Redwater Reef, Alberta

Taher M. Sodagar and Dr. Don C. Lawton

ABSTRACT

The objective of this study is to analyze and undertake seismic modeling of CO_2 saturation of the Devonian Leduc reservoir characterization at the Redwater reef by using Gassmann fluid substitution seismic modeling. This method was applied to the available wells inside the reef. Zero-offset synthetics were created for these wells before and after fluid substitution.

A distinct P-wave velocity decrease occurs from 0% to about 40% of CO_2 saturation. From around 40% to 100% of CO_2 saturation, the P-wave velocity starts increasing slightly, while the S-wave velocity increases almost linearly with the CO_2 saturation increase. There are slight changes in amplitudes between the wet in-situ reservoir reflections and the fluid substitution modeling reflections of Leduc formation. A time shift is observed at the base of the Leduc reservoir. The maximum time shift at the base of the Leduc reservoir and the highest amplitude difference changes are recognized at around 40% of CO_2 saturations.

INTRODUCTION

The Alberta Basin is one of the Canada's largest petroleum sedimentary basins and is one of the world's largest commercial opportunities for reducing CO_2 emissions into the atmosphere. It could be done through Carbon Capture and Storage (CCS) in the subsurface deep geological formations (Gunter and Bachu, 2007). The most emissions of CO_2 are from large stationary sources, such as thermal power plants, refineries, oil sand plants, and cement plants (Bachu, 2000).

There are a few objectives of this study. First objective is to generate synthetic seismograms for the wells that penetrated Devonian Cooking Lake formation inside and around the Redwater reef. Another main objective is to identify and evaluate the future CO_2 saturation in the Devonian Leduc reservoir at the Redwater reef by using fluid substitution seismic modeling. Additional objective of this study is to generate synthetic seismograms with multiples effects before and after fluid substitution for the inside reef wells to evaluate and correlate with the seismic data that coming soon.

AREA OF STUDY

The study area is located in the Redwater region of Alberta northeast of Edmonton, which has Townships of 56 to 58 and Ranges of 20 to 24W4 (Figure 1). The Leduc reef at Redwater is one of the largest Devonian Leduc reefs in Western Canada sedimentary basin (WCSB) and is the third largest oil reservoir in Canada. The Original Oil in Place (OOIP) reserves is about 1.3 billion barrels. The Redwater reef is in the Heartland area close to large sources of CO_2 in the Redwater-Fort Saskatchewan-Edmonton region (Gunter and Bachu, 2007).

The reef complex has a triangular shape (Figure 1) with an area of about 600 km^2 and lies at depth of about 1000 m (-400 m elevation), and has a thickness of 160 to 300 m and had an original oil cap almost 50 m thick. The Redwater reef is currently under the last stages of water flooding for oil production, and this depleted oil reservoir is currently used for water disposal (Bachu et al, 2008).
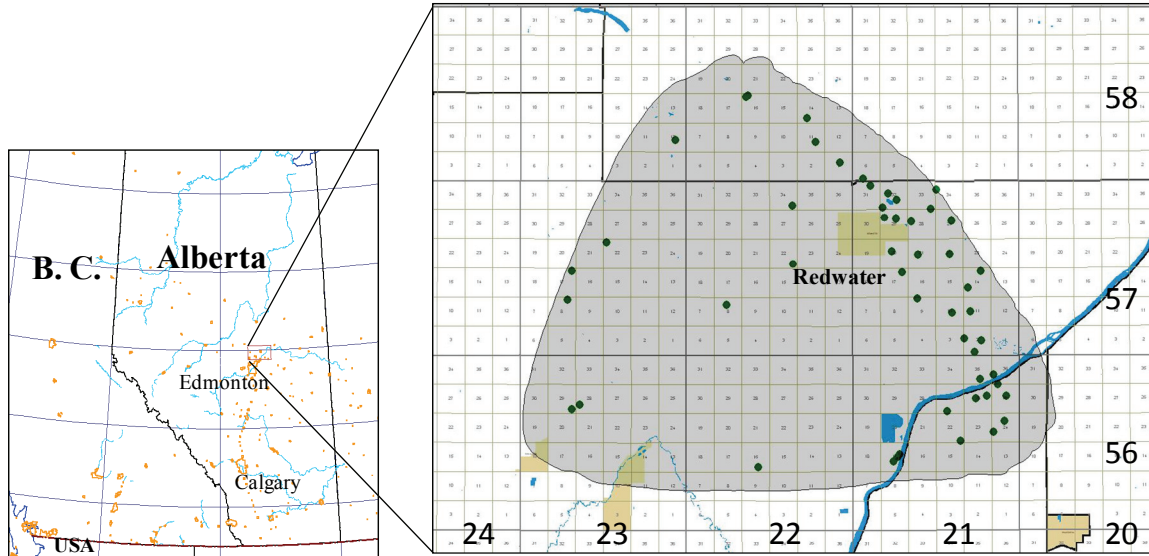

Figure 1: Alberta map showing the location of Study area and the wells penetrating the Lower Leduc formation.

GEOLOGICAL BACKGROUND

Regional Geologic and Stratigraphic Settings

Devonian reefs are present within the (1930 km long and 563 km wide) Western Canadian sedimentary basin (WCSB). The lowlands of the Precambrian shield area formed the eastern limit of the basin, while the Cordilleran miogeosyncline formed the western border (Klovan, 1974).

Three major episodes of reef growth occurred during the Middle and Late Devonian in the WCSB. Each of these episodes is characterized by a comparable pattern of development. Typically, the sequence base is marked by an unconformity (Figure 2), and followed by deposition of widespread shallow-water carbonate platform deposits. Then, biohermal growth develops on this platform. It represents a typical transgressive-regressive sequence of events. The conditions for the reef growth are mainly dependant on depth of water, circulation, and rate of subsidence (Klovan, 1974). A sudden increase in subsidence rate is recorded by the invasion of dark shales into the reef interior (Klovan, 1964). A gradual decrease in subsidence rate is documented by the development of massive stromatoporoid framestone along the seaward edge of the reef complex, and the creation of wide spreading shallow-water, and supratidal deposits in the back reef area.
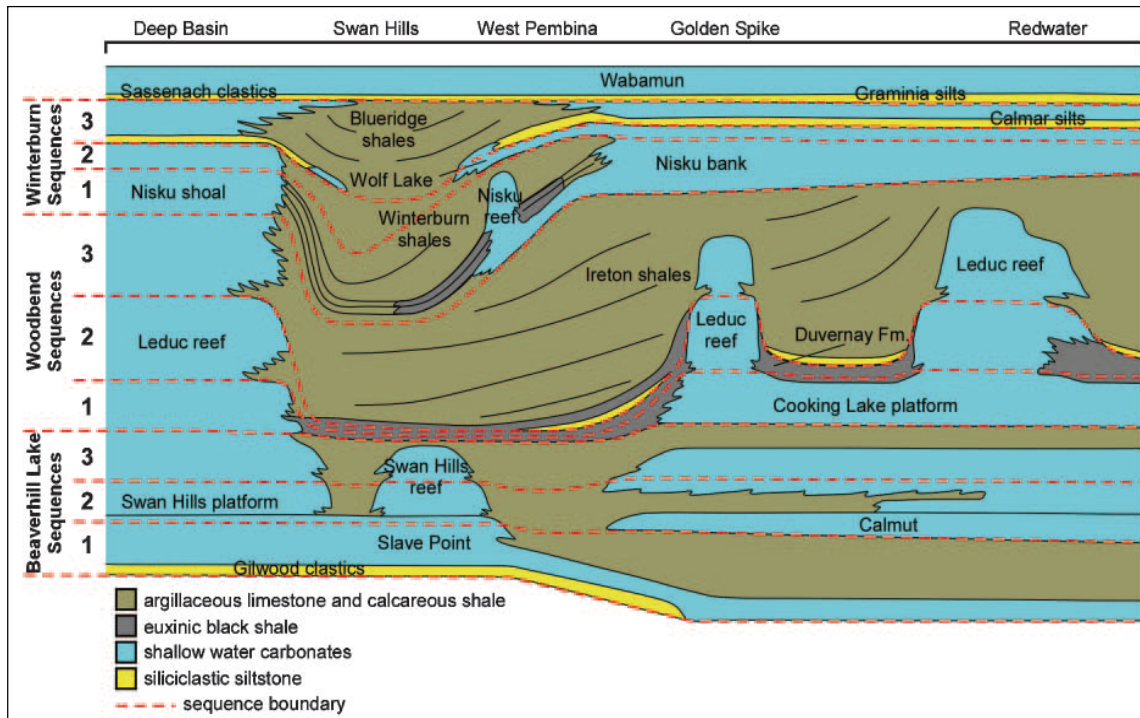
Figure 2: Sequence stratigraphic cross section across central Alberta showing the Devonian sequences and formation subdivisions (from Atchley et al; 2006).

Evolution and Deposition of the Study Area

The study area is located within the Middle to Early Upper Devonian Waterways Basin (Figure 3). It has the deposition of deeper water carbonates and calcareous shales of Beaverhill Lake group. It has an average thickness of 200 m, and usually shows low porosity and permeability (Bachu et al, 2008). The Beaverhill Lake Group is conformably overlain by Cooking Lake shelf platform carbonates, which both dip southwestward. The average thickness of the Cooking Lake Formation reaches up to 90 m and has a reefal margin bordering a shallow basin to the west (Figure 4). Later, the platform growth gradually became differentiated into a number of isolate shoals that formed a depositional high on which following Leduc reef growth took place (Stoakes and Foellmer personal communication, 2008).
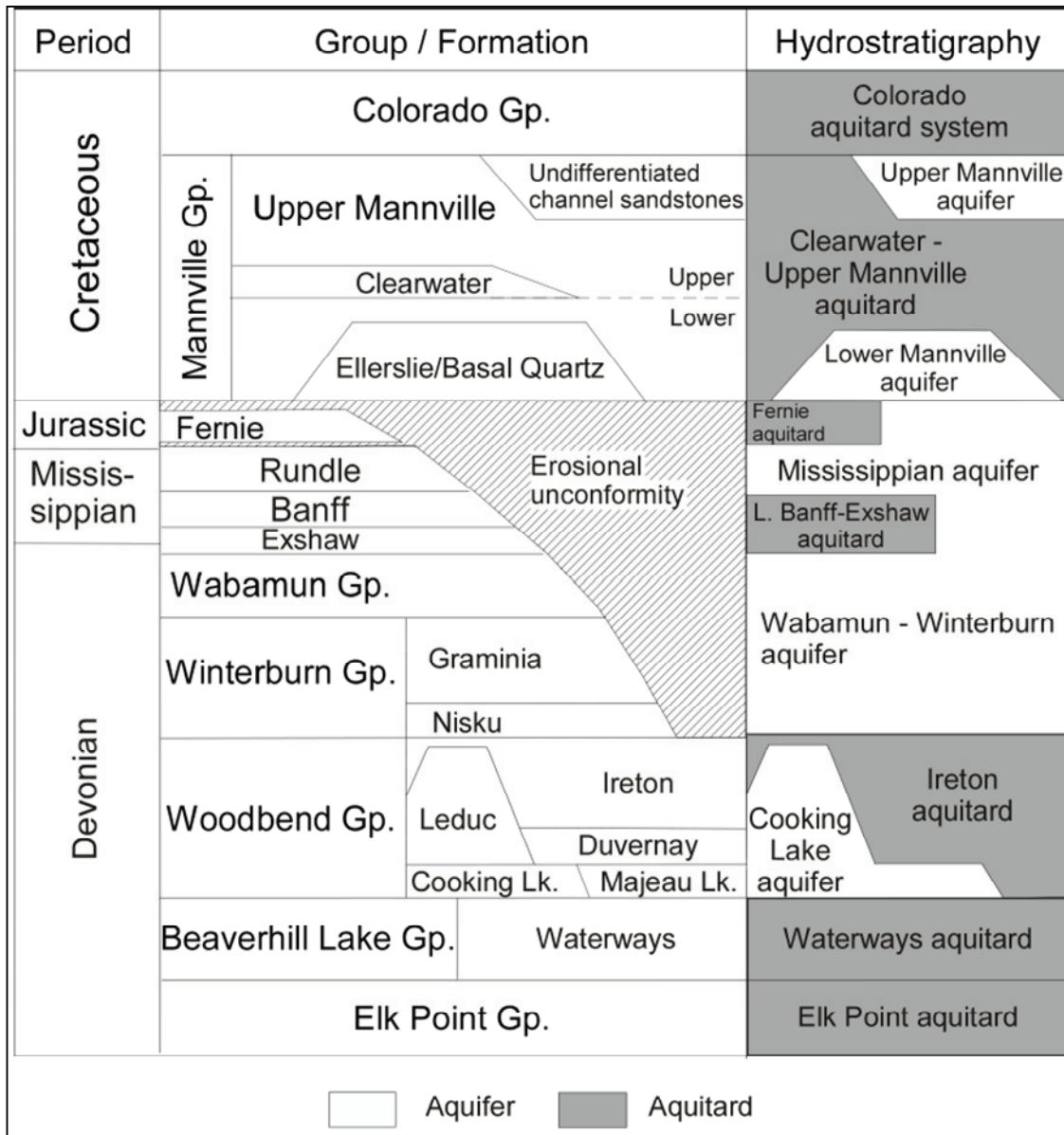
Figure 3: General stratigraphy and hydrostratigrphy presenting the aquifer and aquitard in the study area (Bachu et al; 2008).

Away from the Leduc reef buildup, the Cooking Lake platform is overlain directly by basinal sediments of the interbeded dark brown, organic rich shales, dark brown calcareous shales and dense argillaceous limestones of Duvernay Formation (Figure 5). Thickness ranges from about 70 m in the northeastern part to about 30 m in the west. The Duvernay Formation is overlain by calcareous shales and argillaceous carbonates of the Ireton formation (Figure 5). Its thickness ranges from about 150 m in the East Shale Basin to over 250 m in the southwestern part (Bachu et al, 2008). The Ireton shale formation represents the final infilling of the basin in the study area and works as a regional aquitard and caprock to the oil in the reef reservoir. (Stoakes and Foellmer personal communication, 2008).
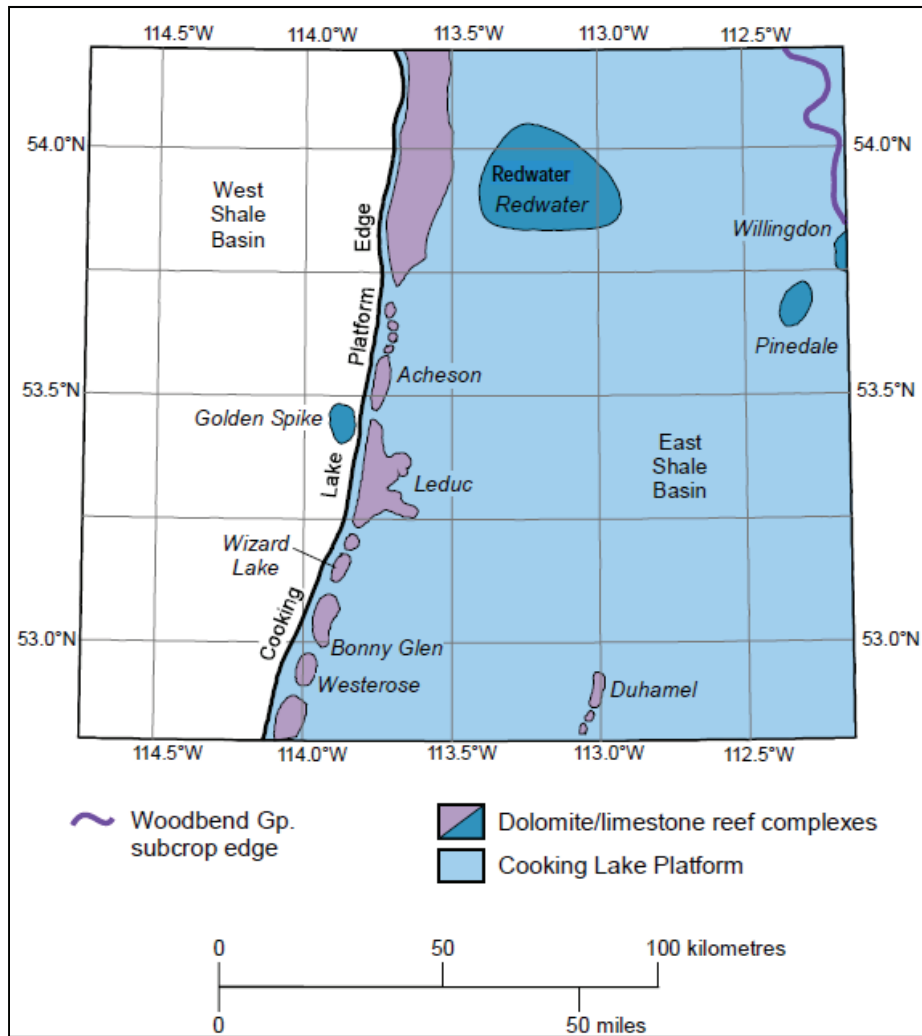
Figure 4: Map of the Cooking Lake platform showing the location of Redwater Leduc reef and Woodbend Group boundaries (Gunter and Bachu, 2007).

The Redwater Reef Facies

The Redwater Leduc reef is capped by shales of the Ireton Formation, which are 10-50 m thick directly above the reef. The reef developed on the Cooking Lake Formation platform carbonates (Bachu et al, 2008) (Figure 4). The Leduc reef total thickness is up to 290 meters and grew as a bulky isolated carbonate atoll surrounded by shallow water. The depositional facies of the reservoir were recognized into foreslope, reef margin and interior lagoon. The Redwater Leduc reef complex was divided into Lower, Middle and Upper Leduc. The marine embayment is the key to differentiate between these subdivisions. The embayment incursion is between Lower Leduc and Upper Leduc sedimentations. The marine embayment presents on the eastern side and the western side with a lesser extent of the reef buildup (Stoakes and Foellmer personal communication, 2008).

Reservoir Quality and Rock Properties

The Devonian Leduc Formation carbonates of Woodbend Group in the Redwater area form a large reefal build-up. The build-up consists mostly of 84% of medium to light-gray fossiliferous limestone, with 15% of minor amounts of secondary, patchy replacement dolomite. In addition, there are traces of iron minerals and anhydrite. The porosity commonly ranges between 1 and 17%, and the average porosity taken from the field is around 7%. (Bachu et al, 2008). Porosity consists primarily of intercrystalline, moldic, and fracture porosity. The permeability ranges from 0.01 to 4000 md (milli-darcy) horizontally and 0.02 to 670 md vertically (Gunter and Bachu, 2007).

Reservoir Pressure and Formation Water

The initial pressure of Redwater pool was 7.4 MPa (coincidentally nearly equal to the CO_2 critical pressure P_c =7.38 MPa) and temperature of $34\,^{o}C$ (a little higher than the CO_2 critical temperature T_c =31.1ºC). The density of formation water in the Cooking Lake aquifer in the study area was 1083 kg/m3 (Bachu et al, 2008). Salinity in the Redwater area ranges from 85 to 140 g/l. The formation water in the reef is NaCl type with 107,000 mg/l TDS (Total Dissolved Solids). The reef experiences a strong water drive from the underlying highly-permeable Cooking Lake aquifer (Bachu et al, 2008).

Hydrogeological Characteristics

The aquifers in the Upper Devonian from Cooking Lake to Lower Cretaceous Lower Mannville sequence show a similar flow pattern on a regional scale. The updip flow from the southwest and downdip flow from the northeast converging into normally northwest channel flow in the Redwater area. The lower hydraulic heads in the Wabamun, Winterburn and Cooking Lake aquifers and the existence of Leduc reefs are suggesting hydraulic communication and downward flow from the Lower Mannville Aquifer into the Cooking Lake Aquifer. The Clearwater Upper Mannville aquitard is an efficient barrier to cross formational flow (Figure 3 and 5). It is hydraulically separating the Upper Mannville Aquifer and the shallower formations from the Lower Mannville aquifer and the deeper underlying Devonian aquifers (Gunter and Bachu, 2007).
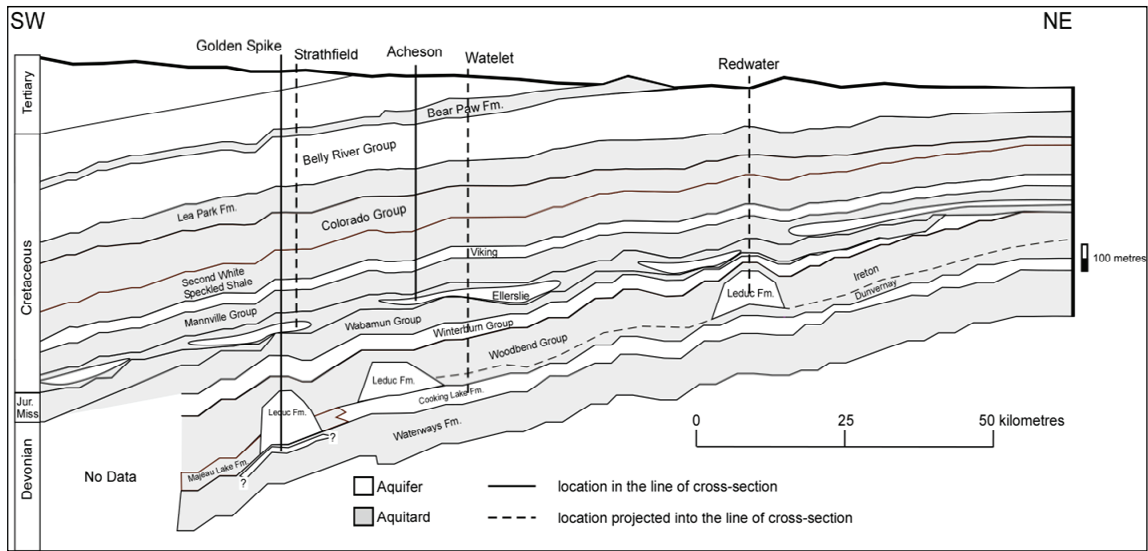
Figure 5: Southwest to northeast dip cross section showing the Redwater reef and also the separation of the Upper Mannville and shallower aquifers from the Lower Mannville and deeper aquifers (Bachu et al, 2008).

METHODOLOGY

Synthetic Seismogram Generation

First step in seismic data interpretation is to correlate the formation tops at well locations from synthetic seismogram to the 2D surface seismic data. Therefore, the first objective of this study is to generate synthetic seismograms for the wells that penetrated Devonian Cooking Lake formation, which is deeper than our target Leduc formation (Figure 6). Six wells have been used to generate zero-offset ray-tracing method synthetics. Only the primary reflection events are modeled, so there are no multiples in consideration. Three wells are inside the Redwater reef and three wells around the reef. GeoSyn Software package is used for generating zero-offset synthetics for these wells. To create synthetics for these wells, P-wave, density, and S-wave logs are used. In our case, there is no S-wave log. Therefore, S-wave log is created using the average of global empirical equations for carbonates in WCSB, which is using a linear equation to relate S-wave and P-wave velocity:

$$V_s = V_p / 1.9$$

where,

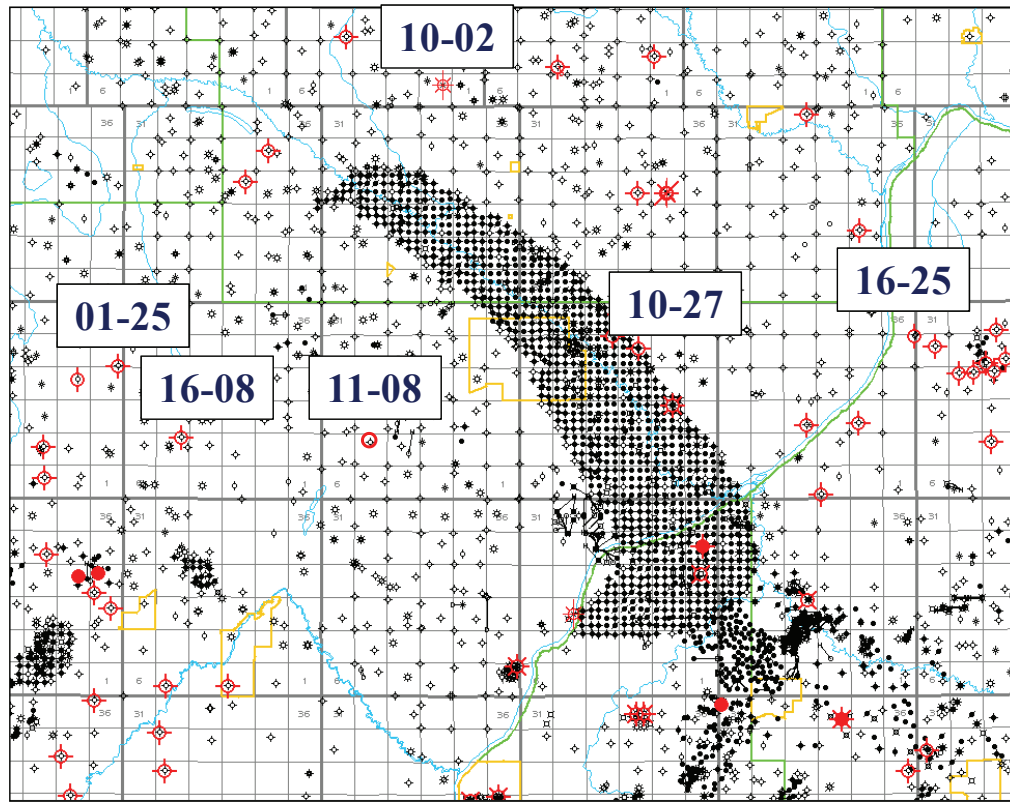V_s is the S-wave velocity, and V_p is the P-wave velocity.

Figure 6: Redwater reef map showing all the wells and all wells that penetrated Cooking Lake formation and have sonic logs in red color. Also, it demonstrates the six wells that synthetics are generated for them.

Fluid Substitution Seismic Modeling

The most common method for fluid substitution modeling is based on Gassmann (1951). He used the rock porosity, the porous rock frame bulk modulus, the mineral matrix bulk modulus, and the pore fluid bulk modulus to calculate the fluid-saturated porous rock bulk modulus (Smith et al., 2003):

$$K_{sat} = K^* + \frac{\left[1 - \frac{K^*}{K_o}\right]^2}{\frac{\emptyset}{K_{fl}} + \frac{(1-\emptyset)}{K_o} + \frac{K^*}{K_o{}^2}}$$

where,

K_{sat} is the saturated rock bulk modulus (un-drained of pore fluids),

K^* is the porous rock frame bulk modulus (drained pore fluid, but not the dry bulk modulus),

K_o is the mineral matrix bulk modulus,

K_{fl} is the pore fluids bulk modulus, and

$\emptyset$ is the rock porosity.

It is expected that shear modulus (μ) of the rock is not affected by fluid saturation, so we assume that:

$$\mu_{sat} = \mu^*$$

where,

μ_{sat} is the saturated rock shear modulus, and μ^* is the porous rock frame shear modulus.

Since the P-wave velocity and bulk density (ρ_b), are measured from well logs, and the S-wave velocity is assumed (Vp/Vs = 1.9), then the saturated rock bulk and shear moduli can be calculated from the following two equations (Smith et al, 2003):

$$K_{sat} = \rho_b [V_p^2 - (4/3) V_s^2]$$
$$\mu_{sat} = \rho_b V_s^2$$

To calculate the porous rock frame bulk modulus, three parameters need to be determined. These are the rock porosity ($\emptyset$), the rock matrix bulk modulus (K_o), and the fluid bulk modulus (K_{fl}). Since the in-situ fluid in the reservoir is the formation water, the density and modulus of the formation water are then 1072 kg/m^3 and 2.8575 GPa respectively. They were calculated using the equations of Batzle and Wang (1992). Also, since the Leduc Formation is a carbonate reservoir, the density, bulk modulus, and shear modulus of the carbonates are then 2736 kg/m^3, 78.96 GPa, and 33.65 GPa respectively, determined from equations by Hashin-Shtrikman (1963). The porosity can be calculated from the equation:

$$\emptyset = (\rho - \rho_m) / (\rho_{fl} - \rho_m)$$

where,

ρ is the measured rock density, ρ_m is the matrix density, and ρ_{fl} is the fluid density.

Now, since the three parameters are known, the porous rock frame bulk modulus can be computed using the backward Gassmann equation:

$$K^* = \frac{K_{sat} \left[\frac{\emptyset K_o}{K_{fl}} + 1 - \emptyset \right] - K_o}{\frac{\emptyset K_o}{K_{fl}} + \frac{K_{sat}}{K_o} - 1 - \emptyset}$$

Finally, the in-situ reservoir fluid can be replaced with CO_2 and therefore, the fluid density and bulk modulus (ρ_{fl} and K_{fl}) can be changed to the new fluid density and bulk modulus. These were calculated by the following equations:

$$\rho_{fl} = \rho_w S_w + \rho_c (1 - S_w)$$
$$1/K_{fl} = S_w/K_w + (1-S_w)/K_c$$

where,

S_w is the formation water saturation,

ρ_w is the formation density,

K_w is the formation water modulus,

ρ_c is the CO_2 density which is 500 kg/m^3 under the reservoir conditions, and

K_c is the CO_2 modulus which is 0.1 GPa under the same condition.

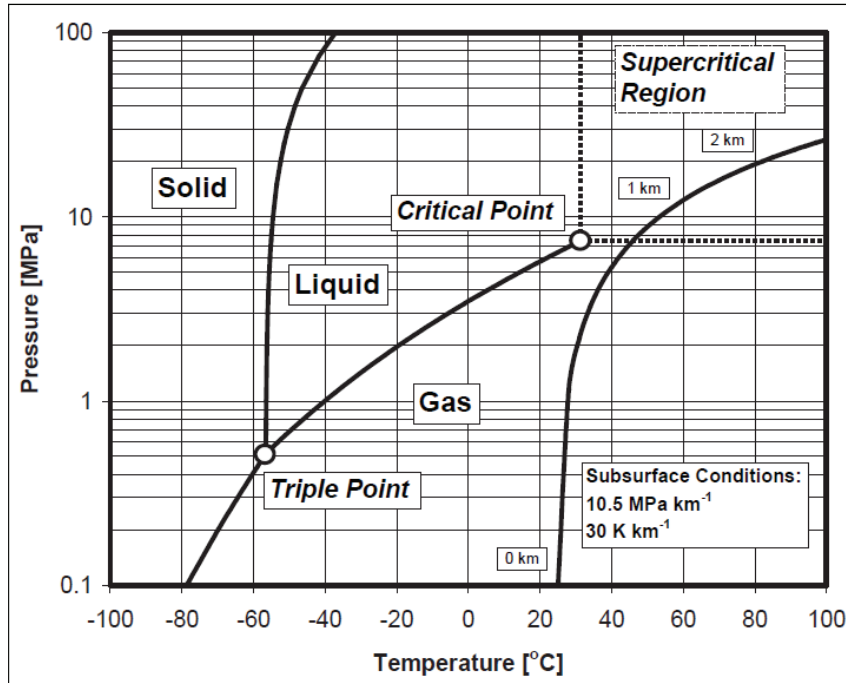CO$_2$ density and modulus were calculated using Batzle and Wang (1992) equations for CO_2 in supercritical phase (Figure 7).

Figure 7: Temperature and pressure phase diagram for pure carbon dioxide (Span et al, 1996, cited by Piri et al, 2005).

Then:

$$K^{new}{}_{sat} = K^* + \frac{\left[1 - \frac{K^*}{K_o}\right]^2}{\frac{\emptyset}{K^{new}{}_{fl}} + \frac{(1-\emptyset)}{K_o} + \frac{K^*}{K_o{}^2}}$$

and the new bulk density (ρ_b) with the new fluid can be obtained from:

$$\rho_b{}^{new} = \rho_{fl} \emptyset + \rho_m (1-\emptyset)$$

To acquire the new P-wave velocity and S-wave velocity after fluid substitution, we apply these equations:

$$V_p{}^{new} = \sqrt{\dfrac{K^{new}{}_{sat} + \frac{4}{3}\mu_{sat}}{\rho_b{}^{new}}}$$

$$V_s{}^{new} = \sqrt{\dfrac{\mu_{sat}}{\rho_b{}^{new}}}$$

There are several assumptions in the application of Gassmann's equations. Firstly, the rock is assumed to be homogeneous. Secondly, all the pores are in communication, and thirdly, the pores are filled with a frictionless fluid. Fourthly, the un-drained rock-fluid system is assumed to be closed, and the pore fluid will not soften or harden the rock frame (Wang, 2001).

RESULTS

Six wells have been used to generate zero-offset synthetic seismograms (Figure 6). Three wells are inside the Redwater reef. They are 10-27-57-21W4 (on the east edge of the reef), 11-08-57-22W4 (in the center of the reef), and 16-08-57-23W4 (on the west edge of the reef). The other three wells are around the reef. They are 16-25-57-20W4 (east side of the reef), 01-25-57-24W4 (west side of the reef), and 10-02-59-22W4 (north side of the reef). The reef wells have Leduc formation (Figures 8 and 9) but the outside wells have not. In all of these wells, shale Ireton formation has trough seismic signature and carbonate Cooking Lake formation has peak signature, but has a very strong seismic peak in the wells outside the reef. This is because the Cooking Lake carbonate overlain by Ireton shale which gives a big seismic contrast. The Leduc formation in the reef wells gives a fairly good seismic peak shape due to fair contrast in P-wave velocity between Ireton shale and Leduc carbonate.

Two wells have been used for fluid substitution seismic modeling. These wells are 11-08-57-22W4 (in the center of the reef), and 16-08-57-23W4 (on the west edge of the reef). Gassmann fluid substitution calculations were computed for the entire thickness of the Leduc Formation (from 1119 to 1411 m) for well 16-08-57-23W4. Table 1 shows some of the computed parameters of the full thickness of the Leduc reservoir (292m) before and after fluid substitution. A distinct P-wave velocity decrease occurs from 0% of CO_2 saturation to 40% of CO_2 saturation (Figure 10). From 40% to 100% of CO_2 saturation, the P-wave velocity increases slightly. In contrast, the S-wave velocity again increases almost linearly with the CO_2 saturation (Figure 11).
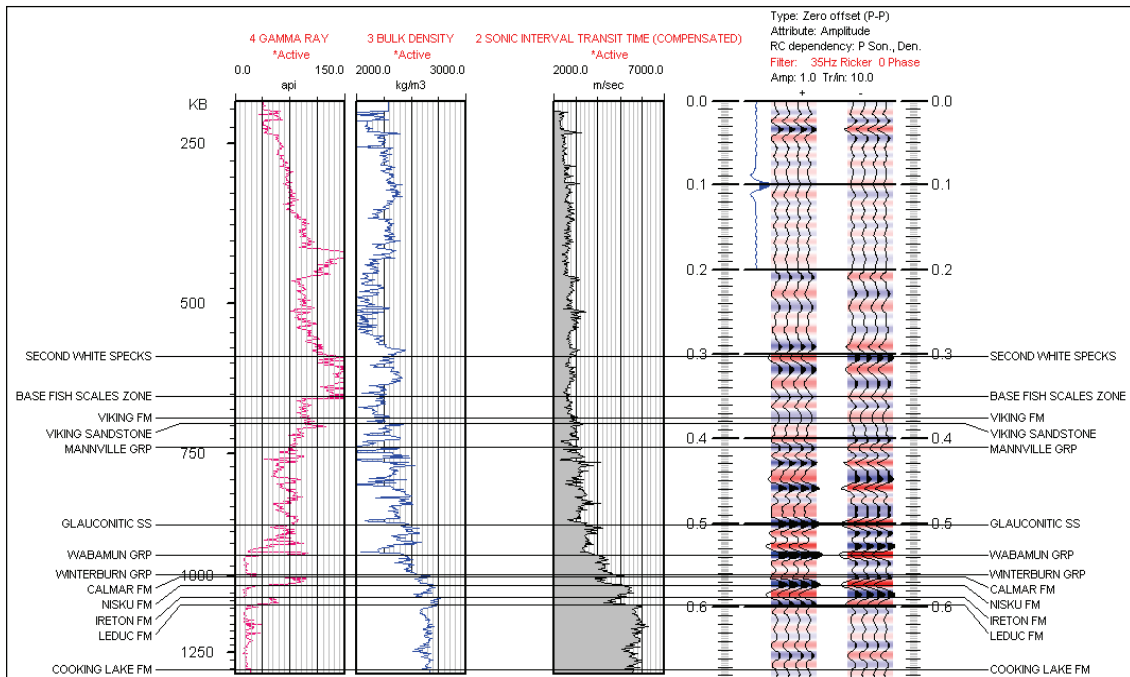
Figure 8: Sonic, density, and gamma ray logs and synthetic of the well 11-08-57-22W4.
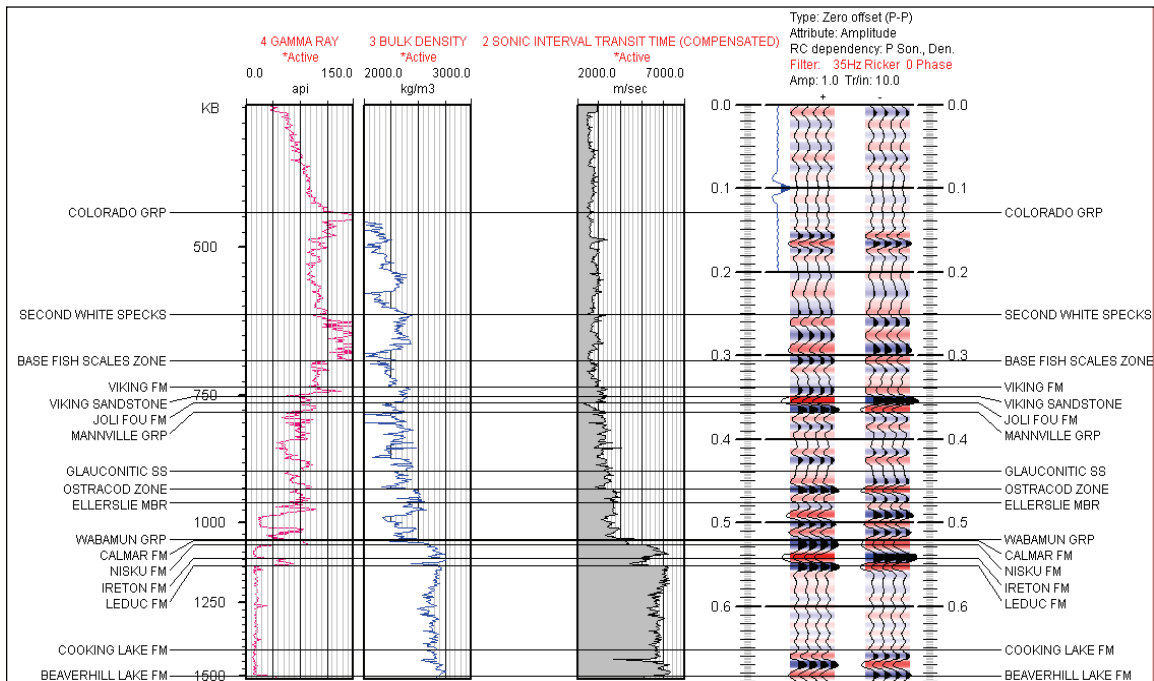

Figure 9: Sonic, density, and gamma ray logs and synthetic of the well 16-08-57-23W4.
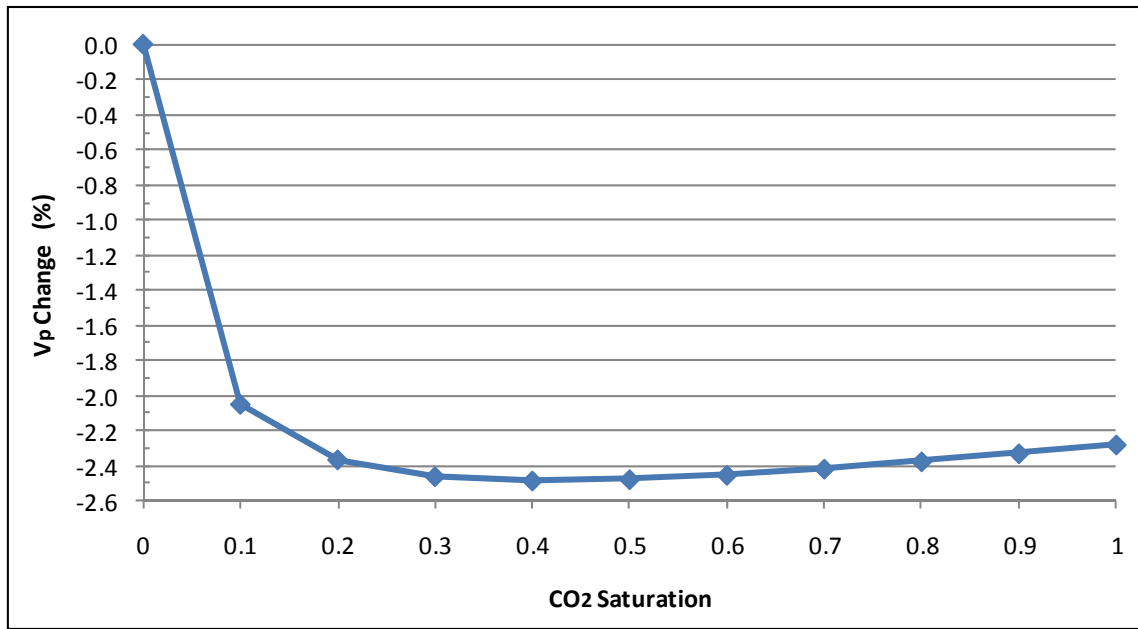
Figure 10: The relationship between the P-wave velocity change and CO_2 saturation for well 16-08-57-23W4.
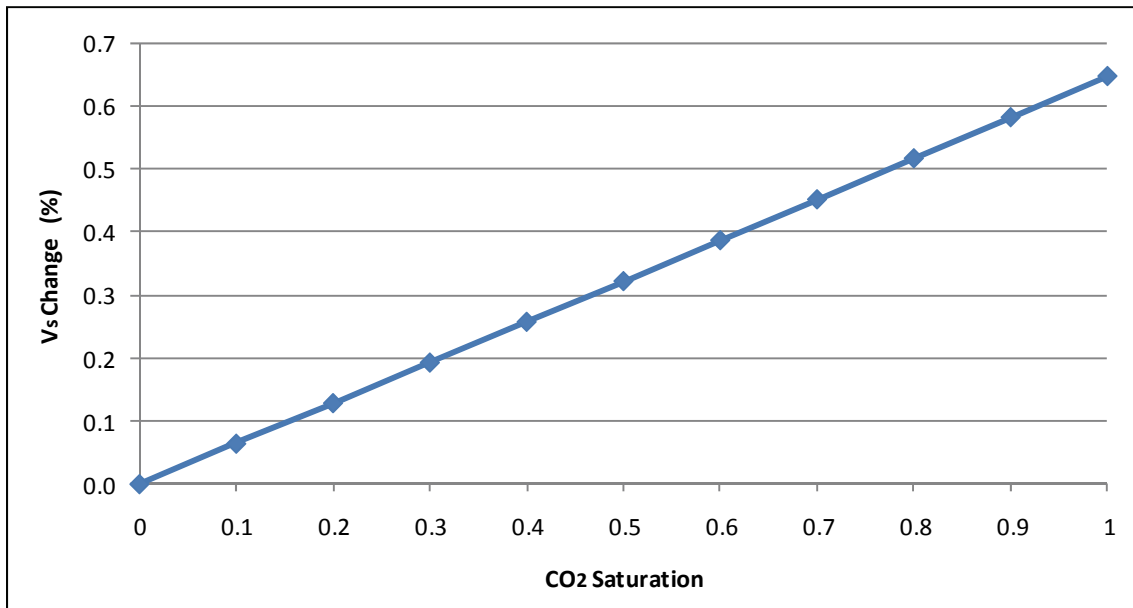

Figure 11: The relationship between the S-wave velocity change and CO_2 saturation for well 16-08-57-23W4.

Table 1: Results of the well 16-08-57-23W4 before and after fluid substitution of various CO2 saturation of the entire thickness of the Leduc formation of average porosity of 5.9%.

CO2 Saturation	Fluid Density (g/cc)	Rock Density (g/cc)	K$_{fl}$ Gpa	K$_{sat}$ Gpa	V$_p$ m/s	V$_s$ m/s	Vp Change %	Vs Change %	Vp/Vs Change %	Δt (ms)
0	1.07	2.64	2.86	55.75	5789	3047	0	0	0	0
0.1	1.02	2.63	0.76	52.05	5670	3049	-2.05	0.06	-2.12	2.1
0.2	0.96	2.63	0.44	51.40	5652	3051	-2.37	0.13	-2.50	2.4
0.3	0.90	2.63	0.31	51.12	5646	3053	-2.47	0.19	-2.65	2.6
0.4	0.85	2.62	0.24	50.97	5645	3055	-2.49	0.26	-2.74	2.6
0.5	0.79	2.62	0.19	50.88	5645	3057	-2.48	0.32	-2.80	2.6
0.6	0.73	2.62	0.16	50.81	5647	3059	-2.46	0.39	-2.83	2.5
0.7	0.67	2.61	0.14	50.77	5649	3061	-2.42	0.45	-2.86	2.5
0.8	0.62	2.61	0.12	50.73	5651	3063	-2.38	0.52	-2.88	2.5
0.9	0.56	2.61	0.11	50.70	5654	3065	-2.34	0.58	-2.90	2.4
1	0.50	2.60	0.10	50.68	5657	3067	-2.29	0.65	-2.91	2.4
Average	0.76	2.62	0.26	51.01	5652	3058	-2.38	0.35	-2.72	2.5

Comparing the native reservoir with 100% of CO_2 fluid fill, a very slight difference is observed in the density. The average bulk rock density changed from 2640 kg/m^3 to 2600 kg/m^3 (about 1.5%) after 100% CO_2 fluid replacement. In addition, the average P-wave velocity decreases by about 2.3% from 5789 m/s to 5657 m/s. In contrast, the average S-wave velocity increases by about 0.65% from 3047 m/s to 3067 m/s, but the Vp/Vs decreases by about 2.9% from 1.9 to 1.84 and the P-wave impedance also decreases by 3.5%. The estimated P-wave two-way time delay caused by CO_2 substitution is about 2.5 ms, calculated using the following equation:

$$\Delta T = T_2 - T_1 = 2 H (1/V_2 - 1/V_1)$$

where,

ΔT is the anticipated two-way time delay caused by CO_2 injection, T_1 and T_2 are the P-wave two-way travel times through the Leduc Formation before and after CO_2 substitution respectively, V_1 and V_2 are the average P-wave velocities of the Leduc Formation before and after CO_2 substitution, respectively, and H is the total thickness of the Leduc formation (292m).

Zero-offset synthetic seismogram was generated for well 16-08-57-23W4 with CO_2 substitutes from 0% to 100% (increasing the CO_2 saturations by 10%). There are slight changes in amplitude between 0% and 40% CO_2 saturation (Figure 12). In addition, there is a subtle velocity reduction with increasing CO_2 saturation, shown by a time delay of

the Cooking Lake event. The sensitivity of the synthetic seismograms to CO_2 saturation is more early seen in Figure 13, which show synthetic seismograms (Figure 13 left) and amplitude difference compared to 0% CO_2 saturation (Figure 13 right). As CO_2 saturation greater than 40%, the amplitude difference becomes less sensitive to CO_2 saturation.
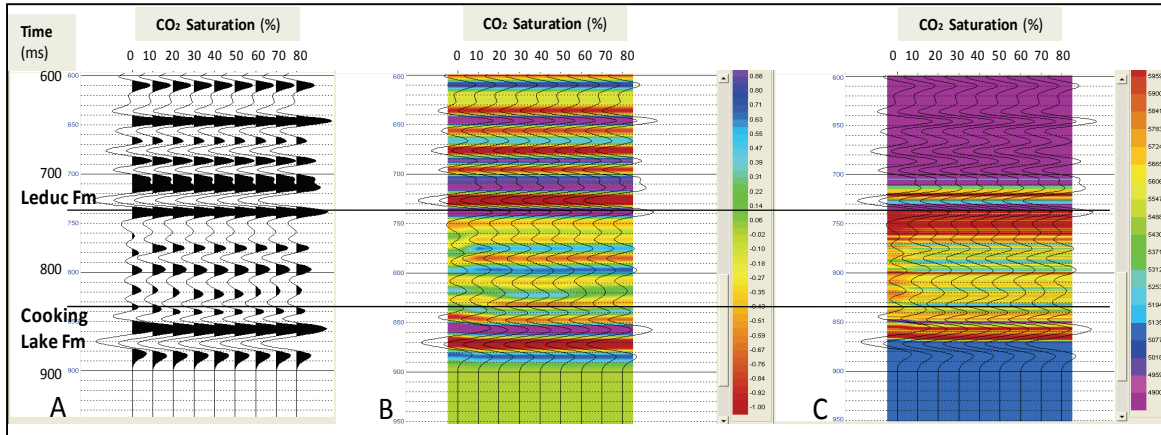

Figure 12: Zero-offset synthetic seismic traces for well 16-08-57-23W4, with CO2 fluid substitution from 0% (left) to 100% (right) in each panel. (A) wiggle-trace display, (B) color amplitude with wiggle-trace overlay, and (C) interval velocity with wiggle-trace overlay.
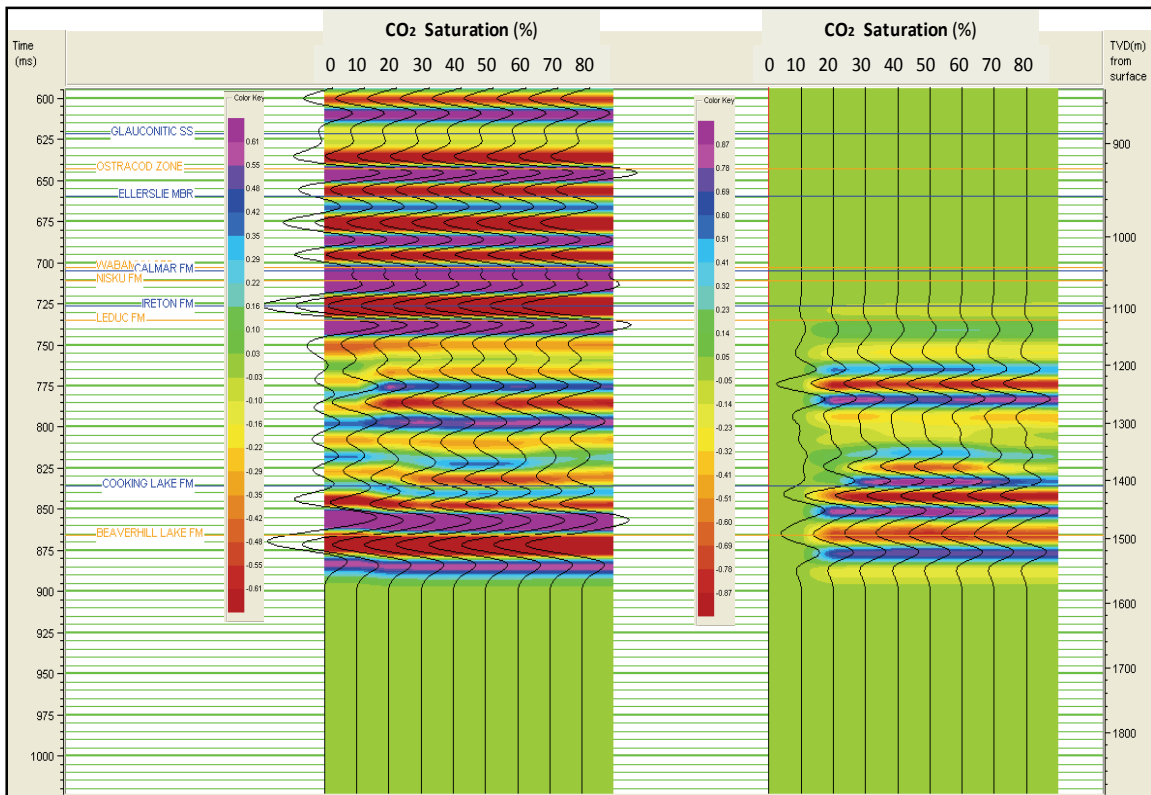

Figure 13: Zero-offset synthetic seismic traces of the well 16-08-57-23W4 before and after fluid substitution. Absolute amplitudes (left), and amplitude difference compared to 0% saturation (right).

In the same way, Gassmann fluid substitution calculations were performed for the entire thickness of the Leduc formation (from 1086 to 1311 m) for the well of 11-08-57-22W4. Table 2 shows some of the computed parameters of the full thickness of the Leduc reservoir (225m) before and after various fluid substitutions. Distinct P-wave velocity decrease occurs from 0% to 40% of CO_2 saturation (Figure 14). From 40% to 100% of CO_2 saturation, the P-wave velocity decreases slowly. In contrast, the S-wave velocity again increases almost linearly with the CO_2 saturation increasing (Figure 15).
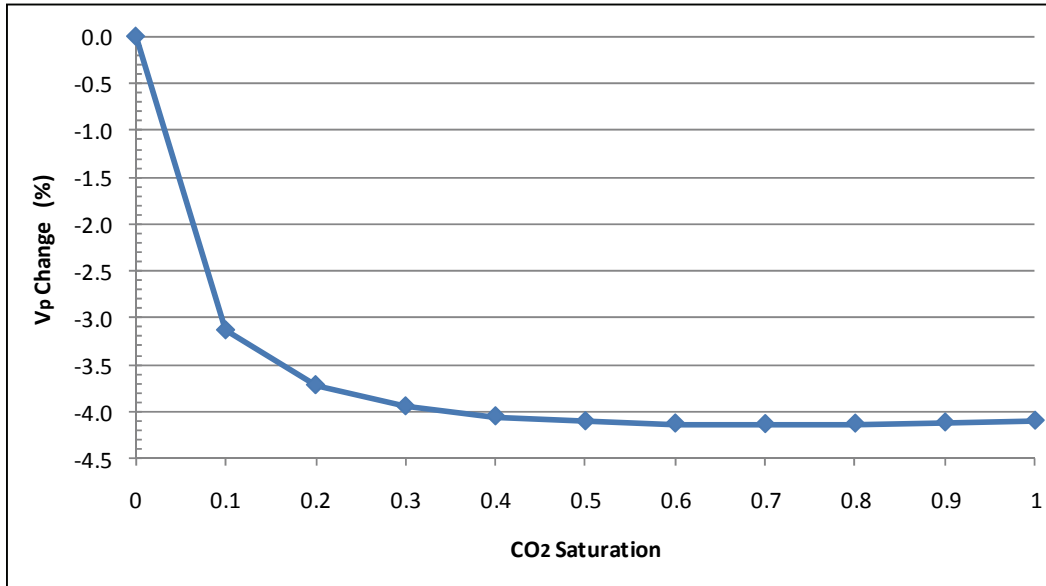

Figure 14: The relationship between the P-wave velocity change and various CO_2 saturations of the well 11-08-57-22W4.
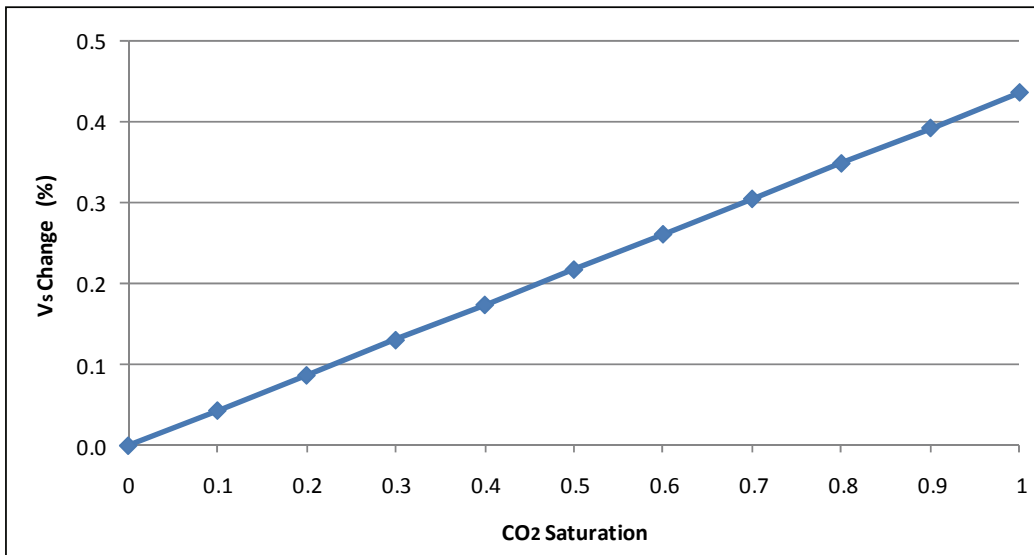

Figure 15: The relationship between the S-wave velocity change and various CO_2 saturations of the well 11-08-57-22W4.

Table 2: Results of the well 11-08-57-22W4 before and after fluid substitution of various CO2 saturation of the entire thickness of the Leduc formation of average porosity of 4%.

CO2 Saturation	Fluid Density (g/cc)	Rock Density (g/cc)	K_{fl} Gpa	K_{sat} Gpa	V_p m/s	V_s m/s	V_p Change %	V_s Change %	V_p/V_s Change %	Δt (ms)
0	1.07	2.64	2.86	55.08	5747	3025	0	0	0	0
0.1	1.02	2.64	0.76	49.61	5567	3026	-3.14	0.04	-3.18	3.3
0.2	0.96	2.64	0.44	48.55	5533	3027	-3.72	0.09	-3.81	3.9
0.3	0.90	2.64	0.31	48.10	5520	3029	-3.95	0.13	-4.07	4.2
0.4	0.85	2.63	0.24	47.85	5514	3030	-4.06	0.17	-4.22	4.3
0.5	0.79	2.63	0.19	47.70	5511	3031	-4.11	0.22	-4.32	4.4
0.6	0.73	2.63	0.16	47.59	5510	3033	-4.13	0.26	-4.38	4.4
0.7	0.67	2.63	0.14	47.51	5509	3034	-4.14	0.30	-4.43	4.4
0.8	0.62	2.63	0.12	47.45	5509	3035	-4.13	0.35	-4.47	4.4
0.9	0.56	2.62	0.11	47.40	5510	3037	-4.12	0.39	-4.50	4.4
1	0.50	2.62	0.10	47.36	5511	3038	-4.10	0.44	-4.52	4.3
Average	0.76	2.63	0.26	47.91	5519	3032	-3.96	0.24	-4.19	4.2

Comparing the in-situ wet reservoir with 100% of CO_2 fluid fill, very slight difference is observed in the density. The average rock density changed from 2640 kg/m^3 to 2620 kg/m^3 (about 0.75% decrease) after 100% CO_2 fluid replacement. In addition, the average P-wave velocity decreases by about 4.1% from 5747 m/s to 5511 m/s. In contrast, the average S-wave velocity increases by about 0.44% from 3025 m/s to 3038 m/s, but the Vp/Vs decreases by about 4.5% from 1.9 to 1.81 and the P-wave impedance also decreases by 4.9%. The estimated P-wave two-way time delay caused by CO_2 substitution is about 4.2 ms.

Zero-offset synthetic seismogram was generated for well 11-08-57-22W4 with CO_2 substitutes from 0% to 100% (increasing the CO_2 saturations by 10%). There are still little changes in amplitudes between the wet reservoir reflections and the fluid substitution modeling reflections of Leduc formation (Figure 16). Also, there are small velocity reductions. Time shift is still observed at the base of the reservoir. The amplitude differences between wet and various CO_2 saturations were performed (Figure 17). The maximum amplitude difference changes are recognized at 40% and 50% of CO_2 saturations. It is observed that there is almost no effect on seismic attributes when limestone or dolomites in mineral compositions are used for fluid substitution for this well.
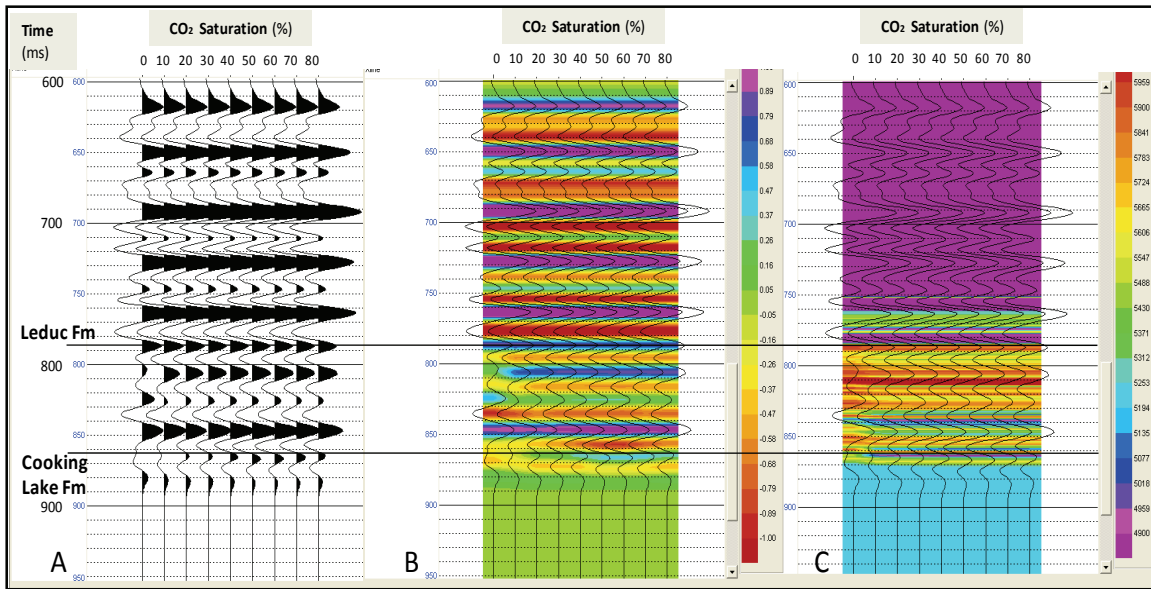
Figure 16: Zero-offset synthetic seismic traces for well 11-08-57-22W4, with CO2 fluid substitution from 0% (left) to 100% (right) in each panel. (A) wiggle-trace display, (B) color amplitude with wiggle-trace overlay, and (C) interval velocity with wiggle-trace overlay.
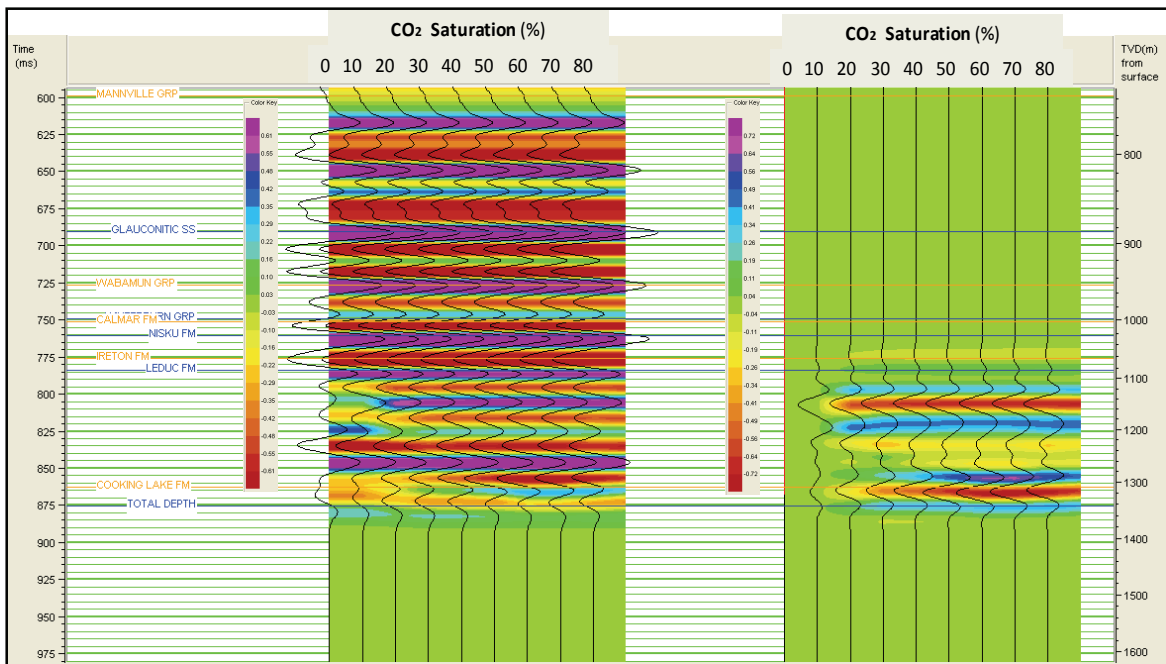

Figure 17: Zero-offset synthetic seismic traces of the well 11-08-57-22W4 before and after fluid substitution. Absolute amplitudes (left), and amplitude difference compared to 0% saturation (right).

After demonstrating the results, some discussions are required about the assumptions that take place during the fluid substitution processes. Firstly, the shear modulus remains constant during the fluid substitution process by using the Gassmann's equation (Smith, 2003). This means that the shear modulus for an isotropic media is independent of pore

fluids, but if the pores are not in communication or cracks happen in the reservoir, this assumption would be dishonored. Secondly, during the fluid substitution process an equilibrium saturation model was assumed. However, during the CO_2 injection, the equilibrium distribution of fluids would be disturbed. Therefore, it would be more sensible and realistic to employ a patchy saturation model rather than the equilibrium saturation model. Moreover, the effects of the pressure, temperature and viscosity variations in the reservoir were not taken in consideration as well.

CONCLUSIONS

Fluid replacement modeling using Gassmann equation is an effective method to model the time lapse differences that caused by the CO_2 injection. For the well 16-08-57-23W4, distinct P-wave velocity decrease occurs from 0% of CO_2 saturation to 40% of CO_2 saturation. From 40% to 100% of CO_2 saturation, the P-wave velocity starts increasing slightly, while the S-wave velocity increases almost linearly with the CO_2 saturation increasing.

The average rock density decreases about 1.5% after 100% CO_2 fluid replacement and the average P-wave velocity decreases by about 2.3%. While, the average S-wave velocity increases by about 0.65%, but the Vp/Vs decreases by about 2.9% and the P-wave impedance also decreases by 3.5%. The estimated P-wave two-way time delay caused by CO_2 substitution is about 2.5 ms.

Zero-offset ray tracing synthetics were generated for the well 16-08-57-23W4 before and after fluid substitution. There are slightly obvious changes in amplitudes between the wet in-situ reservoir reflections and the fluid substitution modeling reflections of Leduc formation. The time shift is obviously observed at the base of the Leduc reservoir. The maximum time shift at the base of the Leduc reservoir and the highest amplitude difference changes are recognized at around 30% and 40% of CO_2 saturations.

Similarly, for the well 11-08-57-22W4, distinct P-wave velocity decrease occurs from 0% to 40% of CO_2 saturation. From 40% to 100% of CO_2 saturation, the P-wave velocity decreases slowly. In contrast, the S-wave velocity increases almost linearly with the CO_2 saturation increasing. The average P-wave velocity decreases by about 4.1% after 100% CO_2 fluid replacement. While, the average S-wave velocity increases by about 0.44%, but the Vp/Vs decreases by about 4.5% and the P-wave impedance also decreases by 4.9%. The estimated P-wave two-way time delay caused by CO_2 substitution is about 4.2 ms.

There are slightly changes in amplitudes between the wet in-situ reservoir reflections and the fluid substitution modeling reflections of Leduc formation. Also, Time shift at the base of the Leduc reservoir and the higher amplitude difference changes are recognized at around 40% and 50% of CO_2 saturations.

ACKNOWLEDGMENT

REFERENCES

Atchley, S. C., West, L.W., and Sluggett, J. R., 2006, Reserves growth in a mature oil field: The Devonian Leduc Formation at Innisfail field, south-central Alberta, Canada: AAPG Bulletin, vol. 90, Number 8, 1153–1169.

Bachu, S., Buschkuehle, M., Haug, K. and Michael, K., 2008, Subsurface characterization of the Edmonton-area acid-gas injection operations: Energy Resources Conservation Board, ERCB/AGS Special Report 092, 134 p.

Bachu, S., 2000, Suitability of the Alberta subsurface for carbon-dioxide sequestration in geological media: Alberta Geological Survey, Alberta Energy and Utilities Board, Earth Sciences Report 00-11.

Batzle, M., and Wang, Z., 1992, Seismic properties of pore fluids: Geophysics, 57, 1396-1408.

Gassmann, F., 1951, Elastic waves through a packing of spheres: Geophysics, 16, 673-685.

Gunter, B., and Bachu, S., 2007, The Redwater Reef in the Heartland Area, Alberta; A Unique Opportunity for Understanding and Demonstrating Safe Geological Storage of CO2: ARC and AEUB Document on Heartland Redwater CO2 Storage opportunities.

Hashin, Z. and Shrikman, S., 1963, A variational approach to the theory of elastic behavior of multiphase materials: J. Mech. Phys. Solids, 11, 127-140.

Klovan, J., E., 1974, Development of Western Canadian Devonian Reefs and Comparison with Holocene Analogues: AAPG Bulletin, vol. 58, Number 5, 787–799.

Klovan, J. E., 1964, Facies analysis of the Redwater Reef complex. Alberta, Canada: Bulletin of Canadian Petroleum Geology, vol. 12, 1-100.

Piri, M., Prevost, J. H., and Fuller, R., 2005, Carbon Dioxide Sequestration in Saline Aquifers: Evaporation, Precipitation and Compressibility Effects: Fourth Annual Conference on Carbon Capture and Sequestration DOE/NETL.

Smith, T. M., Sondergeld, C. H., and Rai, C. S., 2003, Gassmann fluid substitutions: a tutorial: Geophysics, 68, 430-440.

Verwer, K., Braaksma, H., and Kenter, J. A., 2008, Acoustic properties of carbonates: Effects of rock texture and implications for fluid substitution: Geophysics, 73, 51-65.

Wang, Z., 2001, Fundamentals of seismic rock physics: Geophysics, 66, 398-412.